STED nanoscopy with mass-produced laser diodes

Susanne Schrof,[1,4] Thorsten Staudt,[1,4] Eva Rittweger,[1] Nina Wittenmayer,[3] Thomas Dresbach,[3] Johann Engelhardt,[1] and Stefan W. Hell[1,2,*]

[1]German Cancer Research Center / BioQuant, Im NeuenheimerFeld 267, 69120 Heidelberg, Germany
[2]Max Planck Institute for Biophysical Chemistry, Am Fassberg 11, 37077 Göttingen, Germany
[3]Center of Anatomy, University of Göttingen, Kreuzbergring 36, 37075 Göttingen, Germany
[4]These authors contributed equally to this work.
**shell@gwdg.de*

Abstract: We show that far-field fluorescence nanoscopy by stimulated emission depletion (STED) can be realized with compact off-the-shelf laser diodes, such as those used in laser pointers and DVDs. A spatial resolution of 40-50 nm is attained by pulsing a 660 nm DVD-diode. The efficacy of these low-cost STED microscopes in biological imaging is demonstrated by differentiating between clusters of the synaptic protein bassoon and transport vesicles in hippocampal neurons, based on the feature diameter. Our results facilitate the implementation of this all-molecular-transition based superresolution method in many applications ranging from nanoscale fluorescence imaging to nanoscale fluorescence sensing.

OCIS codes: (180.1790) Confocal microscopy; (180.2520) Fluorescence microscopy; (100.6640) Superresolution; (140.2020) Diode lasers.

References and links

1. E. Abbe, "Beiträge zur theorie des mikroskops und der mikroskopischen wahrnehmung," Arch. Mikrosc. Anat. Entwicklungsmech. **9**, 413–468 (1873).
2. S. W. Hell and J. Wichmann, "Breaking the diffraction resolution limit by stimulated emission: stimulated-emission-depletion fluorescence microscopy," Opt. Lett. **19**(11), 780–782 (1994).
3. S. W. Hell, "Far-field optical nanoscopy," Science **316**(5828), 1153–1158 (2007).
4. T. A. Klar and S. W. Hell, "Subdiffraction resolution in far-field fluorescence microscopy," Opt. Lett. **24**(14), 954–956 (1999).
5. V. Westphal and S. W. Hell, "Nanoscale resolution in the focal plane of an optical microscope," Phys. Rev. Lett. **94**(14), 143903 (2005).
6. G. Donnert, J. Keller, R. Medda, M. A. Andrei, S. O. Rizzoli, R. Lührmann, R. Jahn, C. Eggeling, and S. W. Hell, "Macromolecular-scale resolution in biological fluorescence microscopy," Proc. Natl. Acad. Sci. U.S.A. **103**(31), 11440–11445 (2006).
7. E. Rittweger, K. Y. Han, S. E. Irvine, C. Eggeling, and S. W. Hell, "STED microscopy reveals crystal colour centres with nanometric resolution," Nat. Photonics **3**(3), 144–147 (2009).
8. K. I. Willig, S. O. Rizzoli, V. Westphal, R. Jahn, and S. W. Hell, "STED microscopy reveals that synaptotagmin remains clustered after synaptic vesicle exocytosis," Nature **440**(7086), 935–939 (2006).
9. R. R. Kellner, C. J. Baier, K. I. Willig, S. W. Hell, and F. J. Barrantes, "Nanoscale organization of nicotinic acetylcholine receptors revealed by stimulated emission depletion microscopy," Neuroscience **144**(1), 135–143 (2007).
10. C. Eggeling, C. Ringemann, R. Medda, G. Schwarzmann, K. Sandhoff, S. Polyakova, V. N. Belov, B. Hein, C. von Middendorff, A. Schönle, and S. W. Hell, "Direct observation of the nanoscale dynamics of membrane lipids in a living cell," Nature **457**(7233), 1159–1162 (2009).
11. U. V. Nägerl, K. I. Willig, B. Hein, S. W. Hell, and T. Bonhoeffer, "Live-cell imaging of dendritic spines by STED microscopy," Proc. Natl. Acad. Sci. U.S.A. **105**(48), 18982–18987 (2008).
12. S. Pezzagna, D. Wildanger, P. Mazarov, A. D. Wieck, Y. Sarov, I. Rangelow, B. Naydenov, F. Jelezko, S. W. Hell, and J. Meijer, "Nanoscale engineering and optical addressing of single spins in diamond," Small **6**(19), 2117–2121 (2010).
13. V. Westphal, M. A. Lauterbach, A. Di Nicola, and S. W. Hell, "Dynamic far-field fluorescence nanoscopy," N. J. Phys. **9**(12), 435 (2007).
14. M. A. Lauterbach, C. K. Ullal, V. Westphal, and S. W. Hell, "Dynamic imaging of colloidal-crystal nanostructures at 200 frames per second," Langmuir **26**(18), 14400–14404 (2010).
15. M. Reuss, J. Engelhardt, and S. W. Hell, "Birefringent device converts a standard scanning microscope into a STED microscope that also maps molecular orientation," Opt. Express **18**(2), 1049–1058 (2010).
16. D. Wildanger, J. Bückers, V. Westphal, S. W. Hell, and L. Kastrup, "A STED microscope aligned by design," Opt. Express **17**(18), 16100–16110 (2009).

#142125 - $15.00 USD Received 7 Feb 2011; revised 29 Mar 2011; accepted 6 Apr 2011; published 12 Apr 2011

17. D. Wildanger, E. Rittweger, L. Kastrup, and S. W. Hell, "STED microscopy with a supercontinuum laser source," Opt. Express **16**(13), 9614–9621 (2008).
18. B. R. Rankin, R. R. Kellner, and S. W. Hell, "Stimulated-emission-depletion microscopy with a multicolor stimulated-Raman-scattering light source," Opt. Lett. **33**(21), 2491–2493 (2008).
19. V. Westphal, C. M. Blanca, M. Dyba, L. Kastrup, and S. W. Hell, "Laser-diode-stimulated emission depletion microscopy," Appl. Phys. Lett. **82**(18), 3125–3127 (2003).
20. V. N. Rai, M. Shukla, R. K. Khardekar, and H. C. Pant, "A picosecond optical pulse-generator to calibrate the optical streak camera," Rev. Sci. Instrum. **66**(5), 3125–3130 (1995).
21. T. A. Klar, S. Jakobs, M. Dyba, A. Egner, and S. W. Hell, "Fluorescence microscopy with diffraction resolution barrier broken by stimulated emission," Proc. Natl. Acad. Sci. U.S.A. **97**(15), 8206–8210 (2000).
22. M. Dyba and S. W. Hell, "Photostability of a fluorescent marker under pulsed excited-state depletion through stimulated emission," Appl. Opt. **42**(25), 5123–5129 (2003).
23. A. Fejtova and E. D. Gundelfinger, "Molecular organization and assembly of the presynaptic active zone of neurotransmitter release," in *Results and Problems in Cell Differentiation* (Springer-Verlag, 2006), pp. 49–68.
24. M. Shapira, R. G. Zhai, T. Dresbach, T. Bresler, V. I. Torres, E. D. Gundelfinger, N. E. Ziv, and C. C. Garner, "Unitary assembly of presynaptic active zones from Piccolo-Bassoon transport vesicles," Neuron **38**(2), 237–252 (2003).

1. Introduction

Due to its sensitivity and ability to image the interior of cells, far-field fluorescence microscopy has become one of the most widely applied methods in modern life sciences. Its popularity has grown despite the fact that its resolving power has been restricted by the wave nature of light [1]. However, with the advent of stimulated emission depletion (STED) microscopy [2] and more recent techniques [3] allowing conceptually unlimited resolution in the far field, this fundamental obstacle has been overcome. In the last decade, STED microscopy has become a powerful tool for subdiffraction fluorescence imaging [4–7] that has been increasingly applied in the biological as well as in the material sciences [8–12].

STED microscopy overcomes the diffraction barrier by using stimulated emission to transiently turn off the capability of fluorophores to emit spontaneously. This transient fluorescence silencing is utilized to make features, that are closer than the diffraction barrier, fluoresce sequentially in time. This is typically accomplished by overlapping a regularly focused excitation beam with a doughnut-shaped STED beam (featuring a point of minimal intensity at the center) that instantly de-excites fluorophores to the ground state. Thus the doughnut minimum defines the spatial coordinate at which the fluorophores are still active [2]. The fluorescence capability of markers located elsewhere in the excitation spot is prohibited because the high probability for stimulated emission disallows the fluorophore to assume the fluorescent state. As a result, the fluorophore spends virtually all the time in one of its dark states, meaning that it is switched off. The subdiffraction extent of the region in which fluorescence is allowed defines the resolution; it is given by $\Delta r \approx \lambda / \left(2n \sin\alpha \sqrt{1 + I/I_s} \right)$ [5,7], with I being the intensity at the doughnut crest. $I_S = h\nu/(\sigma\tau)$ is the threshold intensity at which the fluorescence ability is reduced to 50%, with $h\nu$ being the photon energy, σ the cross-section for stimulated emission and τ the fluorescent lifetime. The wavelength of light is denoted by λ and the numerical aperture of the lens by $n \sin\alpha$.

Since in STED microscopy, as in all RESOLFT-type nanoscopy techniques, the detection coordinate is predefined by the light pattern (e. g. by the doughnut) any measured photon can be assigned to this predefined position. This targeted on-off switching and read out allows fast, in practice up to several 100 frames per second recording rates, depending on the brightness of the sample [13,14]. Thus, STED delivers subdiffraction images without mathematical post processing of the recorded data. Moreover, because stimulated emission is a basic transition, potentially any bright and stable fluorescent marker can be employed for STED. On the other hand, because stimulated emission has to act on the relatively short-lived fluorescent state ($\tau \approx$1-5 ns), for efficient fluorescence silencing, the rate for stimulated emission has to be higher than the relatively fast spontaneous decay rate $1/\tau$. This results in values of I_s of the order of a few MW/cm^2 making a strong laser source essential for high resolution STED imaging.

While the initial pulsed STED systems provide outstanding resolution, they were so complex and uneconomical in use that their wide use was severely hampered. A step toward simpler implementation has been made by the realization of dedicated phase plates

#142125 - $15.00 USD Received 7 Feb 2011; revised 29 Mar 2011; accepted 6 Apr 2011; published 12 Apr 2011

transforming the STED beam into a doughnut-shaped focal intensity distribution, while leaving the excitation beam unaffected [15,16]. By exploiting supercontinuum lasers [17] or stimulated-Raman-scattering sources [18] compact and flexible STED setups have been implemented. However, the repetition rate of these systems (1MHz) yields relative slow acquisition rates. Fiber based laser sources are easy to maintain, but semiconductor laser technology promises even greater robustness and cost-efficiency due to lower complexity. Westphal et al. applied diode lasers to STED microscopy [19], but the laser power was limited so that only a resolution enhancement of a factor of two was achieved.

Relevant for the resolution in STED microscopy are the maximal intensity and the quality of the intensity minimum of the STED beam, i.e. the contrast between the central doughnut minimum and the doughnut crest. Consequently, the ideal STED light source features an excellent beam quality paired with high intensity, preferably operated in a pulsed mode with a repetition rate of several megahertz (for fast recording times) and pulse durations of 0.3-1 ns (for efficient fluorophore silencing). While for a long time it seemed that this demand can be met only with mode-locked Ti:sapphire or mode-locked gas laser based systems, here we show that competitive STED performances can be achieved using compact, off-the-shelf laser diode modules, in fact by laser pointers and lasers used in DVDs.

2. Setup and materials

2.1 Laser diode as STED light sources

First, we tested a simple continuous wave (cw) laser pointer at 660nm with 200mW output power as the STED light source (Class 3b laser, 20 €, DealExtreme, Hong Kong). Already with this simple laser a lateral resolution of 80-90nm could be realized which is more than twice the confocal resolution. A laser operated in the pulsed mode yields higher peak intensity than in cw operation when operating at the same average power. In this way the photons can be used more effectively for STED, yielding a higher resolution. Typically pulsed laser diodes are used in fluorescence lifetime measurements for which subnanosecond time resolution is essential. These short pulses are commonly generated in an external optical resonator or by injecting a modulated current in the laser diode which require expensive systems and components. To operate the laser diode in the nanosecond regime, in our experiments a simple laser diode driver based on the same concept as the one described by Rai et al. [20] proved to be sufficient.

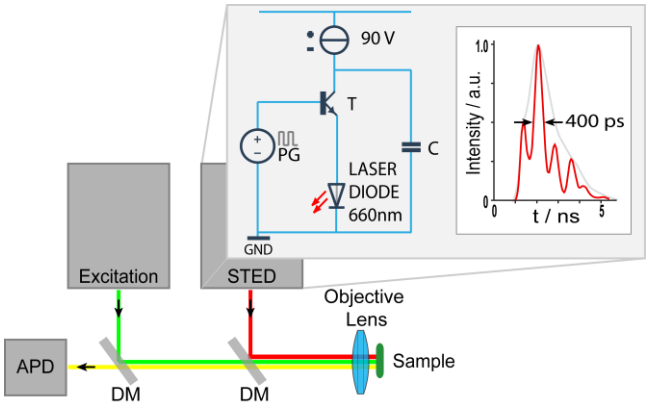

Fig. 1. Employing a DVD laser diode as light source for STED. Setup including the schematic diagram of the electrical driver circuit for the laser diode and the intensity profile of the generated pulses. T: transistor, C: capacitor, PG: pulse generator, GND: ground; DM: dichroic mirror; APD: avalanche photodiode.

In order to build today's simplest and possibly most economic laser suitable for STED, we resorted to a 660 nm off-the-shelf laser diode (130 mW, HL6545MG, opt next, Japan), a standard component in DVD-drives. We controlled its electrical pumping system for pulsed mode operation using standard electronic components. The estimated peak power lies in the

#142125 - $15.00 USD Received 7 Feb 2011; revised 29 Mar 2011; accepted 6 Apr 2011; published 12 Apr 2011

range of 0.5-1 W, which is a 4-7-fold increase compared to the laser power in cw operation. The principle layout of the electrical pulse circuit is shown in Fig. 1. It is based on three main components: a bipolar transistor T (BFG19S), a capacitor C = 20pF and a constant current source. The circuit is triggered by an external pulse generator (TG4001, TTi, Forth Worth, TX). The constant current source charges the capacitor linearly up to 80V. The transistor acts as a switching element and is operated in the avalanche mode. It becomes conductive upon triggering of the pulse generator, which causes the capacitor to discharge within <1 ns. As a result, the laser diode is driven by a short current pulse. The pulse repetition rate of the laser diode is set by the pulse generator and was kept constant at 5 MHz in all STED experiments reported here in order to compromise between short acquisition times and sufficiently high peak intensities.

Figure 1 shows a typical intensity profile of the optical pulses which was measured with a photomultiplier (H7422-40, Hamamatsu, Tokyo, Japan) and time-correlated single photon counting (HydraHarp 400, PicoQuant, Berlin, Germany). The pulses consist of a central peak and several sidelobes. The damped relaxation oscillations are caused by changes in the pump power during the switching process in the electrical pulse circuit. Mainly the central maximum contributes effectively to STED and is therefore here referred to as the STED pulse. To disallow the fluorescent state by the presence of the stimulating photons, the STED pulses have to be significantly longer than the lifetime of the higher vibrational level of the ground state into which the molecule is stimulated, but shorter than the lifetime of the fluorescent state τ. Avoiding multi-photon induced bleaching processes also call for longer STED pulses, meaning that pulse durations in the range from a hundred picoseconds to about 1 ns are optimal for most dyes [21,22]. The measured pulse width of 400 ps, which is a convolution of the actual pulse width and the PMT transition time jitter, shows that the laser diode has sufficiently short pulses. The actual pulse width might be shorter, but it is reasonable to assume that the simple driver will not produce shorter pulses than sophisticated commercial ones with pulse durations in the range of 100 ps. Further optimization of the electrical circuit could possibly reduce the relaxation oscillations.

2.2 Description of the optical setup

A pulsed laser diode at 532 nm (PicoTA, Picoquant, Berlin, Germany) serves as the excitation source which was triggered by the STED pulses of the 660 nm laser diode (see above). The two beams are combined by a dichroic mirror and coupled into a microscope stand (DMI 4000B, Leica Microsystems GmbH, Mannheim, Germany) equipped with a three axis piezo stage-scanner (PI, Karlsruhe, Germany) and an oil immersion lens (ACS APO, 63x/1.30NA, Leica Microsystems GmbH, Mannheim, Germany) which also imaged the fluorescence signal onto a confocally arranged aperture of a photon counting module (SPCM-AQR-13-FC, PerkinElmer, Canada). The doughnut shaped intensity profile of the STED focus was generated by inserting a phase plate (RPC Photonics, NY, USA) which induced a helical phase ramp from 0 to 2π on the initially flat wave front.

2.3 Additional specifications of the STED light source

The wavelength of the laser diode was measured by a spectrometer (Ava-Spec-2048-SPU, Avantes, Broomfield, USA) to be 660 nm with a FWHM of 1.6 nm. The charge injection into the diode was estimated to 1-2nC (~80V · 20pF) per pulse resulting in close to 1nJ light pulses.

2.4 Fluorescent bead sample preparation

Nile red filled polysterene micro spheres (specified diameter 20nm, Invitrogen, Eugene, USA) were sowed on poly-L-lysine coated cover slips and mounted in DABCO containing Mowiol (Fluka, Buchs, Switzerland) to avoid molecular diffusion and reduce photobleaching.

2.5 Neuron sample preparation

Dissociated hippocampal cultures were prepared from E19 Wistar rats and cultured at a density of 60.000 cells / cm^2 on poly-L-lysine-coated cover slips in neurobasal medium

#142125 - $15.00 USD Received 7 Feb 2011; revised 29 Mar 2011; accepted 6 Apr 2011; published 12 Apr 2011

supplemented with B27 and glutamine (Invitrogen, Eugene, USA). Fixation was performed on DIV13 (day 13 in vitro). Bassoon was immunostained using monoclonal antibody sap7f407 (Enzo Life Sciences) and Atto565 (AttoTec, Siegen, Germany).

3. Imaging results

To demonstrate the ability of the pulsed laser diode to silence the spontaneous emission of the fluorophores, we synchronized the STED diode to the 532 nm excitation laser; subsequently both were coupled into a scanning microscope. The confocal image of fluorescent beads shown in Fig. 2 was recorded at constant excitation intensity while the STED beam was interrupted periodically in time. The fluorescence signal from areas with the beam switched on dropped down by 90-95% which is sufficient as 'on-off' contrast for STED microscopy.

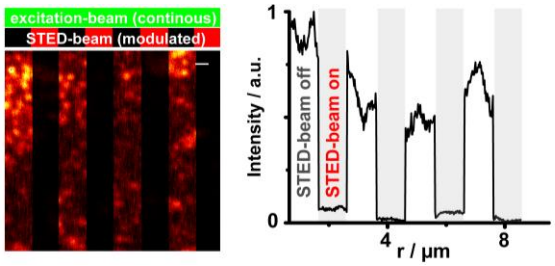

Fig. 2. To demonstrate STED an image of fluorescent beads was recorded at constant excitation but modulated STED-beam (left). The corresponding fluorescence intensity profile of the image (right) shows that when applying STED the fluorescence signal drops down to < 10%.

We exploited this optically induced fluorescence silencing of the fluorophore for subdiffraction microscopy by producing a doughnut-shaped intensity distribution in the focal plane which keeps all molecules non-fluorescent except those in close proximity to the center

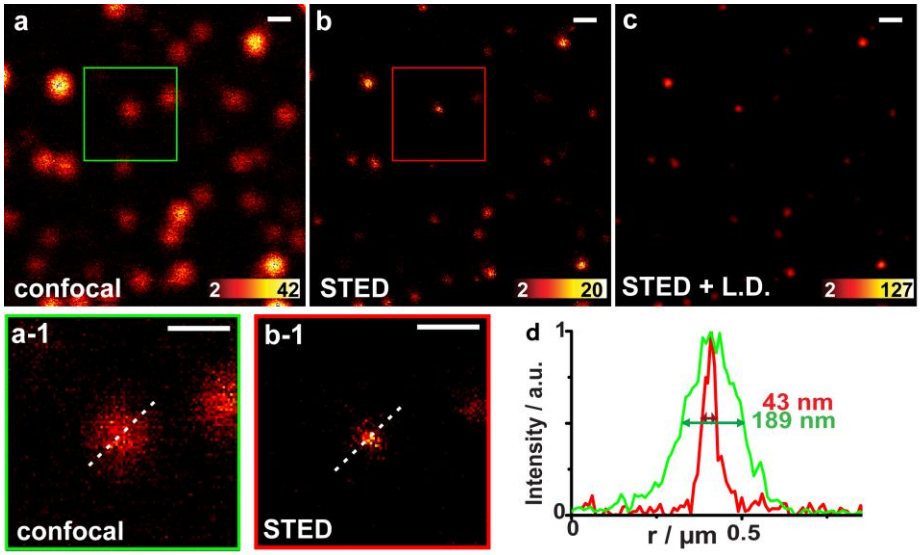

Fig. 3. STED imaging with the compact and simple laser diode: (a) confocal image of Nile red fluorescence beads and corresponding STED images ((b) raw data and (c) linear deconvolution) (a-1), (b-1) Magnified view of the boxed region in (a) and (b). (d) The corresponding line profiles of confocal (green) and STED mode (red) highlight a more than 4-fold resolution gain. Bar size corresponds to 250 nm.

of the 660 nm beam. A measurement of the STED intensity distribution showed a proncounced depth of the doughnut minimum. Therefore no spatial filtering was required. The comparison between the confocal and STED images of fluorescent beads (Fig. 3)

#142125 - $15.00 USD Received 7 Feb 2011; revised 29 Mar 2011; accepted 6 Apr 2011; published 12 Apr 2011

demonstrates a more than 4-fold improvement over the confocal resolution, namely a resolution of 40-50nm in the STED mode.

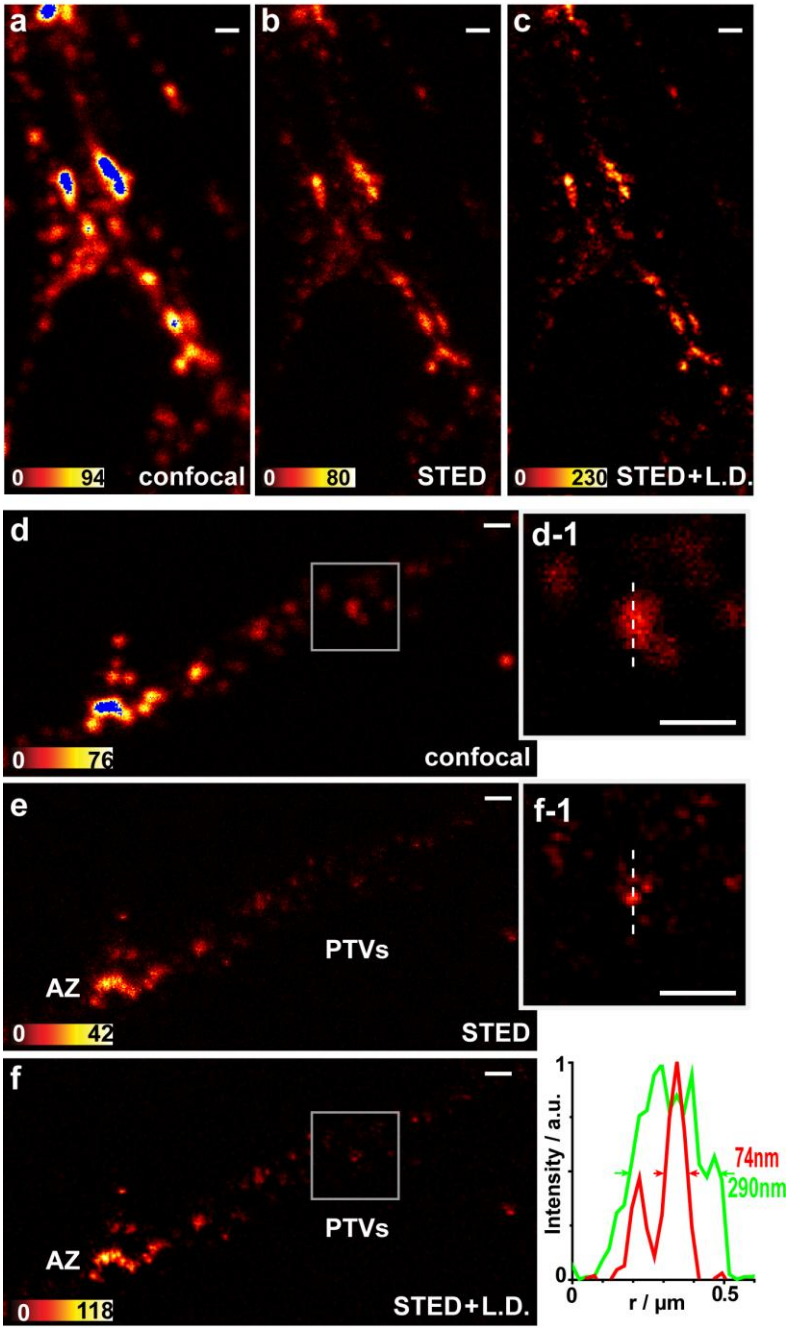

Fig. 4. Presynaptic active zone protein Bassoon in hippocampal-neurons. (a),(d) Confocal image, (b), (e) STED raw data, and (c), (f) STED data linearly deconvolved. Magnified views of the boxed region in (d) and (f). The line profiles through these corresponding structures illustrate the resolution gain in the STED mode. Through the enhanced resolution of STED the active zone (AZ) and bassoon/piccolo transport vesicles (PTVs) can be distinguished by their different diameters. Bar size corresponds to 500 nm.

To show the applicability of our pulsed laser diode based STED system to biological imaging we immunostained and imaged the synaptic protein bassoon in cultured rat

#142125 - $15.00 USD Received 7 Feb 2011; revised 29 Mar 2011; accepted 6 Apr 2011; published 12 Apr 2011

hippocampal-neurons. Bassoon is a multi-domain protein which is specifically localized at the presynaptic active zone and predicted to be involved in cytomatrix organisation and neurotransmitter release [23]. Figure 4 compares the confocal with the corresponding STED images of bassoon in cultured neurons. The subdiffraction resolution provided by STED enables the discrimination between bassoon clusters at the presynapic active zone and bassoon/piccolo transport vesicles having a typical diameter of about 70-90 nm [24].

In conclusion, we have realized a compact and simple STED system based on a off-the-shelf (DVD) laser diode yielding a lateral resolution of 40-50 nm. This compact and low-cost implementation will increase the availability of STED and facilitate turning it into a commonly used tool. In the near future, further simplification is planned by also replacing the excitation light source with a simple and economic laser diode. Moreover, the presented STED light sources provide the opportunity to easily convert existing confocal laser scanning microscopes into STED nanoscopes with subdiffraction resolving power.

Acknowledgments

We acknowledge Jay Jethwa for critical reading. The project has been supported by the German Federal Ministry of Education and Research (BMBF, 13N11173).

#142125 - $15.00 USD Received 7 Feb 2011; revised 29 Mar 2011; accepted 6 Apr 2011; published 12 Apr 2011